INTERNATIONAL JOURNAL OF
MULTIDISCIPLINARY STUDIES IN ARCHITECTURE AND
CULTURAL HERITAGE

VOLUME 4, ISSUE 2, 2021, 99 – 122.

Utilization of Paraloid / Titanium dioxide nanocomposite in the Consolidation of Archaeological Bone

Mostafa Samir Abo El-Hassan

Conservator, Ministry of Tourism and Antiquities, Egypt

Mohamed Marouf

Conservation Department, Faculty of Archaeology,
Sohag University, Egypt

Wael Sabry Mohamed

Polymers and Pigments Department, National Research Centre,
Dokki, Giza, Egypt

Abstract

There are some archaeological bones resulting from some archaeological excavations, and they have many different manifestations of damage such as brittleness, fragility and weakness, and through the aging of some samples that have been strengthened with In this study, nano-hydroxyapatite concentrations of 1% and 2% + nano-paraloid concentration of 3% dissolved in acetone as an archaeological bone-strengthening substance . Visual assessment and several analytical techniques were used for the evaluation of the selected strengthening material .The analytical techniques are transmission electron microscope (TEM), color change and Pressure strength. The results obtained from transmission electron microscope showed that grain size of nano- Titanium Dioxide with nano paraloid was ranging from 51 to 73 nm.

INTERNATIONAL JOURNAL OF
MULTIDISCIPLINARY STUDIES IN ARCHITECTURE AND
CULTURAL HERITAGE
VOLUME 4, ISSUE 2, 2021, 99 – 122.

Visual assessment proved that nano- Titanium Dioxide 2% with nano paraloid had some simple changes in appearance. Color change revealed that nano- Titanium Dioxide 2% with nano paraloid gave the level of total color differences (ΔE) after thermal and chemical aging with 2.46 and 2.96 respectively compared to the standard sample TI2 gave 4.91 . The Pressure strength revealed that nano- Titanium Dioxide 2% with nano paraloid after thermal and chemical aging gave Pressure strength 70.65 kg/cm2 and 100.15 kg/cm2 respectively compared to the standard sample ST gave 70 .86 kg/cm2 . According to these results, we recommend the use of nano- Titanium Dioxide 2% with nano paraloid in joining of archaeological Bone ..

Key words

Nano-Titanium Dioxide , Density , Water Absorption , FTIR, Chemical Aging .

1. INTRODUCTION

Consolidation is an important process in the conservation of various materials including wood. Application of synthetic resin solutions is a generally accepted consolidation technique for wood, since a solid polymer can fully or partially fill the voids resulting from degradation, thus repairing the material's integrity and improving its physical and mechanical characteristics [1-2] . The development of new materials and methods for consolidation to improve the efficiency of treated materials is a subject of worldwide interest in conservation research [3] . reported that even though wood consolidated by synthetic and natural chemicals has considerably greater strength than unconsolidated wood, it can still be impaired by fungi, molds or insects due to factors such as wood morphology, chemistry of the consolidant, and location of the consolidant in treated bone.

The development of modern materials and methods for consolidating the artifacts is considered the subject of global interest in research conservation. Moreover, these Consolidation treatments are the most hazardous preservation actions because of the inability to retrieve consolidated materials [4] . The use of synthetic resins in preservation for artifacts is associated with good handling properties, flexibility, and transparency [5] .Consolidants should not alter the object's chemical or optical appearance [6].

Paraloid B-72 is stable and non-yellowing acrylic resin chemically is a copolymer of ethyl methacrylate and methyl acrylate with a molar ratio of approximately 70-30%. It can be applied for bone conservation [7]. It has been applied extensively in conservation as a archaeological bone. B-72 gives excellent mechanical properties and hardness without the brittleness and other disadvantages of higher molecular weight resins [8, 9]. Paraloid B-72 is very stable against water, alkalis, acids, oils and chemical fumes. The layers are very elastic [10] . B72 soluble in Acetone, Amyl Acetate, n-Butanol, Cellosolve, Diacetone Alcohol, Dimethyl Formamide, Ethyl Alcohol, Ethylene Dichloride, Isopropanol, Methylene Chloride, Methyl Ethyl Ketone, Toluene, Trichloroethane and Xylene. B72 is insoluble in White Spirit [7, 11]. The alcohol dispersions may be milky. However, they make clear, coherent films [10, 12]

Nano-sized titanium dioxide has demonstrated its efficiency in many application fields, such as its water repellent effect [13] . Improving the inherent hydrophobic character of a polymer is highly desired as it can promote their protection efficiency against the deterioration effects, which are inducing by humidity. Therefore, the addition of nanoparticles achieves this purpose [14] .

Water repellent polymer-nanoparticle composite can be used for the protection and preservation of surfaces of the cultural heritage [15] . Titanium dioxide nanoparticles were used with a Paraloid B72 to improve its mechanical properties, obtain a transparent, chemically stable, and non-yellowing coating [16] .

The research reported in this paper was aimed at the preparation and characterization of new formulations of an acrylic consolidant based on Paraloid B72 and containing TiO2 nanoparticles. The present research was carried on seven bone samples treated with three consolidating products applied by brushing. This study aims to examine the efficiency of polymeric nanocomposites in the treatment and preservation of pottery objects. Besides, investigate and compare the effect of the application of the consolidation material. Moreover, evaluating the changes in a certain pottery sample property before and after artificial aging. The overall aim is to the establishment of the best strategy for the conservation of this type of cultural objects in museums and archaeological sites.

2. Materials

2.1. Preparation of Bone *samples*

Archaeological bones samples of sheepwere collected from El-Hawawish excavations in Akhmim, sohag, situated at a distance of 12 km from east and north east the city of sohag. This site dates back to the late period, that is about 2000 B.C. After the process of applying Nano Hydroxyapatite with Nano -paraloid, thermal aging was carried out at a temperature of 120 ° C for 10 hours, according to several previous studies carried out by: (Wang, et al, 2010[17],. Hiller, 2003[18],. Kalsbeek and Richter, 2006[19],. Figueiredo, 2010 [20],.

Abd el-Maksoud, 2010[21]), and Chemical aging was performed by immersing the samples in a solution of hydrochloric acid (Sigma-Aldrich, Schnelldorf, Germany) At a concentration of 3% in distilled water for a period of one month , according to several previous studies for: (Kalsbeek and Richter, 2006,. Figueiredo, et al, 2012 [22],.Walker, 2011 [23]), In order to evaluate the Nano- paraloid material and compare the samples before and after the aging processes treated for the samples treated of the Nano Hydroxyapatite 1,2% with Nano -paraloid concentration 3% , The samples were divided into 7 samples: a standard sample (ST), a sample treated with 3% nano-paralloid (Ti1)(Ti2), a treated and thermally aging sample (Ti1H)(Ti2H), and a chemically aging treated sample (Ti1K)(Ti2K).

2.2. Preparation of Nano Parloid B 72/HA nanocomposits.

Paraloid B72 was prepared as a co-polymer of methyl methacrylate/ethyl acrylate (MMA/EA) monomers (Aldrich, Darmstadt, Germany) with a composition ratio of 70/30. It was prepared by solution polymerization technique with solid content 3% as a pure copolymer . The polymerization was carried out according to the following procedure: in a 250-mL three-nicked flask, the desired amount of the monomers with the selected composition ratio (70/30 MMA/EA), was stirred with Acetone for 30 min at room temperature using a mechanical stirrer (500 rpm). In addition, the presence of 0.01 g, 0.02 g of TiO2 nanoparticles (nanopowder، < 100 nm particle size (BET), 99.5% trace metals basisobtained from Sigma-Aldrich, Schnelldorf, Germany). Then, the mixture was heated to 80 ºC.

Then، the initiator potassium persulphate (PPS) (0.27 g) (Sigma-Aldrich, Schnelldorf, Germany) dissolved in 50mL of Acetone and Sodium dodecyl sulphate (SDS) as emulsifier dissolved in 45 mL of Acetone was added to the reaction mixture under continuous stirring for 3 h to obtain the solutions of Paraloid B72/ HA nanocomposites. The concentration was selected based on Bone nature and porosity [24] .

3. Methods

3.1.1. Transmission electron microscope (TEM) .

The TEM images were obtained by a JEM-1230 electron microscope operated at 60 KV (JEOL Ltd., Tokyo, Japan). Prior to examination, the sample was diluted at least 10 times by water. A drop of well-dispersed diluted sample was then placed onto a copper grid (200-mesh and covered with a carbon membrane) and dried at ambient temperature. This procedure was conducted at the National Research Centre in Dokki –Egypt.

3.1.2. Fourier-Transform infrared Spectroscopy (FTIR)

Fourier-Transform infrared Spectroscopy (FTIR) was done with an infrared spectrophotometer, the device model is (FTIR.B RUKER, Alpha, made in German), in the range of 4000 - 400 cm-1, in transmission mode. The analysis was performed at the Chemistry Laboratory, Faculty of Science, Sohag University, and the analysis was done after grinding about less than a gram of the sample and adding 0.1 grams (KBR).) and mix them and then compress them together into a hard disk.

3.1.3. Measurement of Mechanical Properties.

Samples were prepared with dimensions of (3 x 2 x 2 cm), The mechanical properties (compression) test was carried out with a Galdabini-Quasar 600-made in Italy and measured in N/mm2 The working conditions (Load Range: 10000N, Extension Range: 10mm, Speed: 50 mm / min, Endpoint: 5.0 mm, preload: 1.0N). The test was conducted at the Antiquities Restoration Center at the Grand Egyptian Museum, Al-haram, Giza، Egypt.

3.1.4. Measurement of physical properties (Color Change CIE Lab, Density, Porosity and Water Absorption).

- *Measurement of Color Change (CIE Lab) :*

An Optimatch 3100 ® from the SDL Company was used to measure color change. This procedure was carried out at the National Institute of Standards, Al-haram, Giza، Egypt.

- *Density*

Density = ((g) mass)/((cm3) volume) [25-26] :

m2 x h x i

Where radius (n) = 0.50 cm

And the height (p) = 3 cm, and the value (i) = 3.14

The volume = 3.14 x 3 x $(0.50)2$ = 2.3561 cm3.

- *Porosity*

(A.P) in % was defined in the following Equation: [27-28]

$$A.P = \frac{W_2 - W_1}{V} X\ 100 = \%$$

Where: W1 and W2 is dry and wet weight in g and V is the volume in cm3

- *Water Absorption*

(W.A) in % was determined in the following Equation :

$$W.A = \frac{W_2 - W_1}{W_1} X\ 100 = \%$$

Where: W1 and W2 is dry and wet weight in g [29].

3.1.5.

3.1.6. Fourier Transform Infrared Spectroscopy analysis (FTIR).

Bone samples were analyzed using an infrared spectrophotometer Nicolet 380 FT-IR .

4. Results and Discusstion

4.1. Transmission electron microscope (TEM)

From the images, it is clear thatthe particle size of nano Paraloid B-72 ranged between 51 and 73 nm. The image also shows that the prepared nano paraloid has spherical shape nano particles with uniform morphology (Fig. 1). Where nanostructures represent a stage of matter between agglomerated molecules and structures and are typically characterized by a large surface area that affects their physicochemical properties [30].

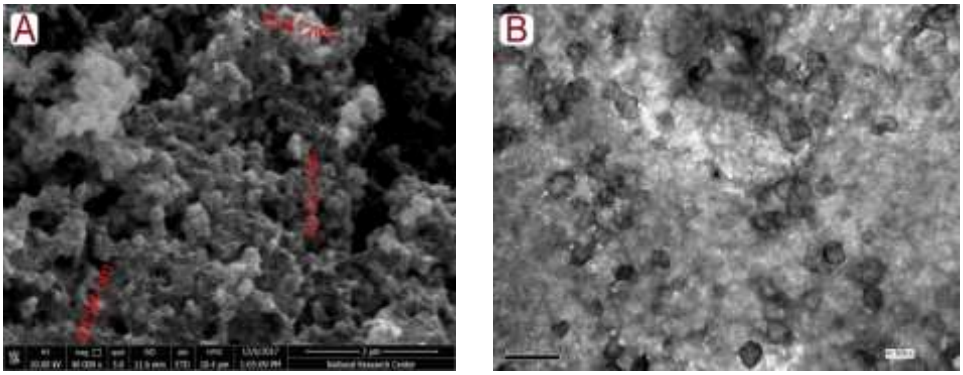

Fig (1) Shows the TEM images of nano Paraloid B-72/TiO2 Nanocomposition . (A) paraloid in nano/TiO2 Nanocomposition form at 3 nm, (B) paraloid in nano/TiO2 Nanocomposition form at 0.2 nm.

4.2. Fourier-Transform infrared Spectroscopy (FTIR).

FTIR is a common tool in characterizing the surface chemical composition. In this study, it is clear that, the characteristic peaks of Nano Paraloid B-72 as C H stretching (2,900–3,000 cm−1), ester carbonyl stretching (C O) at 1,720 cm−1, C H bending at 1,445 and 1,383 cm−1, while (O H) stretching peak appears in the range of 3,400–3,520 cm−1 and stretching of C O C ester bonds from 1,200 to 1,132 cm−1 have been appeared [31, 32]. CH3 rocking vibration were found at the wavelength number of 758, 836, 858 and 968 cm-1, respectively .

INTERNATIONAL JOURNAL OF
MULTIDISCIPLINARY STUDIES IN ARCHITECTURE AND
CULTURAL HERITAGE
VOLUME 4, ISSUE 2, 2021, 99 – 122.

A weak peak located at 1020 cm-1 was the rocking vibration of C–H which was only observed in TiO2/B72. The presence of TiO2 nanoparticles was confirmed by the characteristic peak at 700 – 850 cm−1 [33]. (Fig. 2).

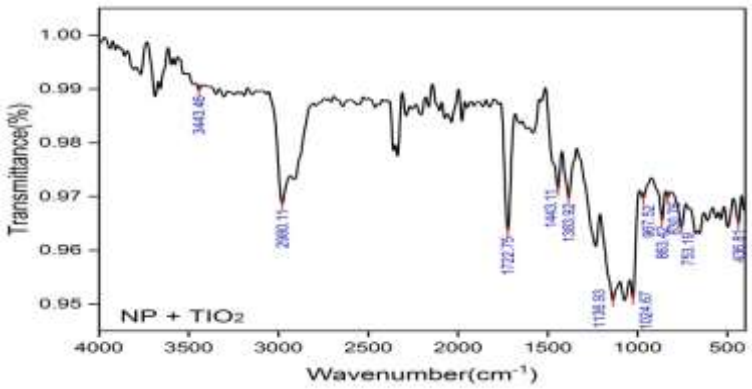

Fig (2) Fourier-Transform infrared Spectroscopy (FTIR) the characteristic peaks of Nano Paraloid B-72/TiO2 nanocomposites

4.3. Measurement of Mechanical Properties .

Table (1) shows the results of pressure tests for nano Titanium Dioxide concentrations of 1,2 % + nano-paraloid concentration of 3%

M	Sample	Stress endurance (kg/cm2)	Stress endurance (N/mm2)
1	ST	70 .86	694.98
2	Ti1	45.46	445.81
3	Ti1H	15.83	155.23
4	Ti1K	7.33	71.94
5	Ti2	130.83	1283.00
6	Ti2H	63.71	624.88
7	Ti2K	52.92	519.03

From the previous table (1) The results of measuring the mechanical properties showed varying changes in the values of the mechanical properties of the samples treated with hardening compared to the standard sample, whether thermally aging samples after hardening or chemically aging samples after hardening. The results came as follows : Where the results of measuring the pressure forces of the reinforced samples and comparing them with the standard sample (ST) (70.86 kg/cm2) resulted in some samples having an increase in the ability to resist pressure forces. Where the reinforcing sample recorded a sample of nano titanium dioxide concentration of 2% (TI2) (130.83 kg / cm2) 130.83 kg / cm², followed by a sample of nano titanium dioxide concentration 1% (TI1) (45.46), and the results of the pressure strength for the thermally aging and hardening samples compared to the standard sample (70.86 kg / cm² (ST), where it was found that some samples happened to A slight effect on the mechanical properties after exposure of samples reinforced with nanomaterials to heat aging, where a sample of nano titanium dioxide concentration 2% (TI2H) recorded (63.71 kg / cm2), followed by a sample of nano titanium dioxide concentration 1% (TI1H) (15.83) The results of the compressive strength of the reinforced and chemically aging samples compared to the standard sample (70.86 kg/cm2) (ST), where it was found that some samples had an increase in mechanical properties and their ability to resist pressure forces compared to the standard sample after exposure to the reinforced samples. nanomaterials for chemical aging Soft nano titanium dioxide concentration of 2% (TI2K) (130.83 kg / cm2), then followed by a sample of titanium dioxide concentration of 1% (TI1K) (7.33 kg / cm2).

4.4. Measurement of Color Change CIE Lab

Table (2) shows the chromatic change values of nano-Titanium Dioxide concentrations of 1,2 % + nano-paraloid concentration of 3%.

M	S	L	A	b	ΔL	Δa	Δb	ΔE
1	ST	52.30	4.11	8.64	-	-	-	-
2	Ti1	65.67	4.40	13.39	13.37	0.29	4.75	14.19
3	Ti1H	48.25	1.71	2.70	-4.05	-2.40	-5.94	7.57
4	Ti1K	61.59	5.93	8.98	9.29	1.82	0.34	9.47
5	Ti2	47.61	-4.69	2.98	-1.13	7.70	-0.94	4.91
6	Ti2H	54.64	2.34	3.93	-0.18	9.40	0.76	2.46
7	Ti2K	52.73	0.43	1.50	-2.61	7.26	-1.38	2.96

From the previous table (2) It is clear that the values of (L) in the sample TI1 were (65.67), as it had a fading as a result of an increase in the values of (L) for the standard sample ST, which was (62.71), while the samples (TI2), (TI1H), (T2H) and (TI2K) And (TI1K), which gave values of (47.61), (48.25), (54.64), (52.73), and (61,59), respectively, it had a slight and moderate darkening compared to the standard sample. As for the values (Δa), the The sample (TI1) and (TI1K) were (0.29) and (1.82), respectively, which gave a color change to the sample to a red color slightly and not noticeably, while the samples (TI1H), (TI2) and TI2H) and (TI2K) which gave values of (-2.40), (-1.13), (-0.18) and (-2.61), respectively, which gave a slight and unnoticeable color change for the samples to green, and for the values (Δb), the sample TI1 was (4.75) gave a change of (4.75).

My color for the sample to yellow color is medium and not noticeable, while samples (TI1K) and (TI2H) gave values of (0.34) and (0.76), respectively, and gave a color change to yellow color very slightly and not noticeably, while samples (TI1H) where were (-5.94) It gave me a moderate and noticeable blue color change, and As for samples ((TI2 and (TI2K)) their values were (-0.94) and (-1.38), respectively, and they gave a slight and unnoticeable color change to blue color

As for the values of (ΔE), the sample TI1 was (14.19) and gave a very large, clear and noticeable total color change for the samples, while the (TI1H) and (TI1K) values gave (7.57) and (9.47) and gave a significant overall color change to the samples and Remarkably, the sample (TI2) had a value of (4.91) and it gave a total color change to the samples in a medium and noticeable manner, while the sample (TI2H) and (TI2K) had values of (2.46) and (2.96), respectively, which gave a total color change for the samples Slightly and unnoticeably.

4.5. Measurement of Physical Properties (Water Absorption, Density, Porosity).

Table (3) shows the chromatic change values of nano-Titanium Dioxide concentrations of 1,2 % + nano-paraloid concentration of 3%.

M	S	Density (g/cm3)	Sample volume before immersion (g)	Sample volume after immersion (g)	Void Volume (g)	Porosity (%)	Water Absorbation (%)
1	ST	3.1133	1.36	1.64	0.28	20.58	17.07
2	Ti1	3.2286	1.96	2.06	0.10	5.10	4.85
3	Ti1H	2.8283	1.52	1.78	0.26	17.10	14.60
4	Ti1K	3.3647	2.00	2.40	0.40	20	16.66
5	Ti2	3.8557	1.84	2.88	1.04	55.52	36.11
6	Ti2H	2.9949	1.62	2.84	1.22	75.30	42.95
7	Ti2K	3.1307	1.75	3.35	1.60	91.42	47.61

From the previous table (3) Which clarified the density of the samples and their comparison with the standard sample (ST), it was found that the samples of nano titanium dioxide concentration of 2% are (TI2), (TI2H) and (TI2K), the results of which were (3.8557 g/cm3) and (2.9949 g/cm3) And (3.1307 g/cm3), respectively, is the highest density compared to the density of the rest of the samples of the other material and compared to the standard sample (3.1133 g/cm3). It is also clear that the 1% concentration of nano titanium dioxide samples gave the lowest rates of porosity compared to the samples of the other material and the standard sample. Where the results of the samples are as follows: it gave the result of sample (TI1) (5.10), while sample (TI1H) (17.10), and sample (TI1K) (20) gave a lower rate than the standard sample in all its samples compared to the standard sample (ST) which recorded (20.58%), as it is clear that the 1% concentration of nano titanium dioxide samples gave the lowest water saturation rates compared to the other material samples and the standard sample. 14.60), and sample (TI1K) (16.66).

4.6. Fourier Transform Infrared Spectroscopy analysis (FTIR).

And through Fig No. (3) shows the components of hydroxyapatite, it appeared in the ranges of 559 and 598 cm-1, which corresponds to the asymmetric bending vibrations of the spectrum of phosphate groups (O-P-O) for 1% titanium dioxide samples in the standard sample ST, as well as samples TI1,TI1H ,TI1K, where there was an increase in the vibration intensity of the TI1K sample, and a decrease in the vibration intensity of the samples TI1H, TI1 compared to the standard sample.

Moreover, the absorption at 1017 cm-1 corresponds to the asymmetric expansion of the O-P-O group, and another band appeared at 1053 cm-1 in all samples. For titanium dioxide 1%, the vibration intensity of the TI1K sample was increased, and the vibration intensity of the samples TI1, TI1H decreased compared to the standard sample. cm-1 in the standard sample in the TI1K sample at the range of 1112 cm-1 and it was not present in the rest of the samples [34].

As for the carbonate groups -CO3, the distinct bands appeared at 870-880 cm-1 (as a single band) and at 1400-1450 cm-1 (as a double band), where they appeared at the 870 cm-1 band, which corresponds to the asymmetric curvature, where an increase in the intensity of Vibration for TI1K sample, and lower vibration intensity for samples TI1H, TI1 compared to the standard sample, and appeared at the ranges of 1410 cm-1 where it corresponds to the stretching of the asymmetric CO3 and CH2 group and 1457 cm-1 where it corresponds to the expansion of the CO3 group and the curvature of the asymmetric CH2 group of the standard sample , where there was an increase in the vibration intensity of the TI1K sample, and a decrease in the vibration intensity of the samples TI1, TI1H compared to the standard sample, this range is characteristic of B-type apatite, thus most of the absorption from the phosphate vibrations is clearly observed in both bone spectra of hydroxyapatite, and it can be observed The doubly degraded mode of hydroxyapatite at less than 500 cm−1 appeared in sample TI1H at the 420 cm−1 range [35].

As for the second component of bone, collagen, the organic component of bone, many vibrational bands originated from the amide groups that form peptide bonds to this protein. , is the strongest adsorption band in collagen, mainly caused by the C = O stretching vibration (with a slight contribution from CN stretching), being found in the 1645, 1649, 1649 and 1645 cm-1 bands for samples ST, TI1, TI1H, TI1K respectively [36].

Amide II, which is present at the 1500-1600 cm-1 range in collagen, is mainly caused by a combination of bending and CN-stretching vibrations of the peptide bonds, being present in the 1551, 1543, 1541 and 1541 cm-1 bands for samples TI1H,TI1,ST, TI1K respectively, and the Amide III band (1200-1300 cm-1) exists mainly from the CN extension and NH curvature, as it is present in the bands of 1274, 1247, 1251, and 1210 cm-1 for samples ST, TI1, TI1H, TI1K respectively, where it occurred An increase in the intensity of vibration for TI1K sample, and a decrease in the intensity of vibration for samples TI1, TI1H compared to the standard sample in all amide bands [37].

The Amide A and Amide B bands are located, close to 3300 cm-1 and 3100 cm-1 respectively, from the extended base band of NH, wherein Amide A is present in the 3284, 3288 and 3274 cm-1 bands for samples ST,TI1H, TI1K and non Its presence in the TI1 sample, and the deteriorating state of collagen can be observed through the loss of amide A in the TI1 sample, and we also notice an extension in the bonds of the main functional groups, which refers to the chemical structure of methylmethacrylate in nano-paralloid (CH), where the bonds extended between 2800 - 3100 cm -1 [38].

Also, the characteristic TI-O group of titanium dioxide, which appears through the characteristic bands at 700-850 cm-1, appeared in TI1 samples at 759 cm-1 and in TI1K sample at 796 cm-1 and not in TI1H sample [33].

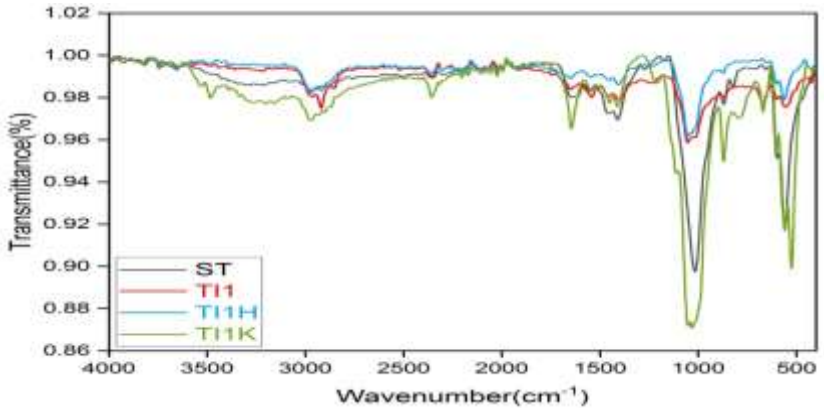

Fig (3) shows FTIR Analysis of nano- Titanium Dioxide concentrations of 1% + nano-paraloid concentration of 3% .

And through Fig No. (4) shows the components of hydroxyapatite, it appeared in the ranges of 559 and 598 cm-1, which corresponds to the asymmetric bending vibrations of the spectrum of phosphate groups (O-P-O) for 2% titanium dioxide samples in the standard sample ST, as well as samples TI2K, TI2H, TI2, where there was a decrease in the intensity of vibration for all samples compared to the standard sample, moreover, the absorption at 1017 cm-1 corresponds to the asymmetric expansion of the O-P-O group, and another band appeared in TI2 sample at wavelength 1055 cm-1, where there was an increase in the intensity of The vibration of the TI2H sample, and a decrease in the vibration intensity of the TI2K, TI2 samples compared to the ST standard sample. TI2 at the range of 1163 cm-1 and not present in the rest of the samples.

As for the carbonate groups -CO3, the distinct bands appeared at 870-880 cm-1 (as a single band) and at 1400-1450 cm-1 (as a double band), where they appeared at a band of 870 cm-1, which corresponds to the asymmetric curvature, as it increased The vibration intensity of the TI2H sample and the decrease of the vibration intensity of the samples TI2K, TI2 compared to the standard sample, appeared at the ranges of 1410 cm-1 where it corresponds to the expansion of the asymmetric CO3 and CH2 group and 1457 cm-1 where it corresponds to the expansion of the CO3 group and the curvature of the asymmetric CH2 group For the standard sample, which had an increase in the vibration intensity of the TI2H sample and a decrease in the vibration intensity of the samples TI2, TI2K compared to the standard sample, this range is characteristic of the B-type apatite, thus most of the absorption from the phosphate vibrations is clearly observed in both the bone spectra of hydroxychloroquine apatite, and the doubly degraded mode of hydroxyapatite can be observed at less than 500 cm-1, as it appeared in the TI2H sample at the 465 cm-1 band.

As for the second component of bone, collagen, the organic component of bone, many vibrational domains originated from the amide groups that form the peptide bonds of this protein. Typically characteristic vibrations of amide groups in collagen, the amide I band located in the 1600-1700 cm-1 range, is the strongest adsorption band in collagen, mainly caused by the C=O stretching vibration (with a slight contribution from CN stretching), Where it is found in the ranges of 1645, 1649, 1647 and 1645 cm-1 for samples ST, TI2, TI2H, TI2K respectively.

Amide II, which is present at the 1500-1600 cm-1 range in collagen, is mainly caused by a combination of bending and CN-stretching vibrations of the peptide bonds, and is present in the 1551, 1541, 1543 and 1541 cm-1 bands for samples ST, TI2, TI2H, TI2K Respectively, the band Amide III (1200-1300 cm-1) exists mainly from the CN extension and the NH curvature, which is present in the range of 1274 cm-1 for the standard ST sample and in the TI2, TI2K sample at the range of 1234 and 1229 cm-1, respectively, and not present. In the TI2H sample, an increase in the intensity of vibration occurred for all samples compared to the standard sample ST in all amide bands.

The Amide A and Amide B bands are located, close to 3300 cm-1 and 3100 cm-1, respectively, from the extended core band of NH, with Amide A present in the 3284, 3286, 3288 and 3292 cm-1 bands for samples ST,TI2, TI2H, TI2K and the degraded state of collagen can be observed through the loss of amide III in the TI2H sample, and we also notice an extension in the bonds of the main functional groups, which refers to the chemical structure of methylmethacrylate in nanoparalloids, namely (CH), where the bonds extended between 2800-3100 cm-1.

The characteristic TI-O group of titanium dioxide, which appears through the characteristic bands at 700-850 cm-1, appeared in TI2 samples at the 759 cm-1 range and in TI2H at the range 755 cm-1 and did not appear in the TI2K sample

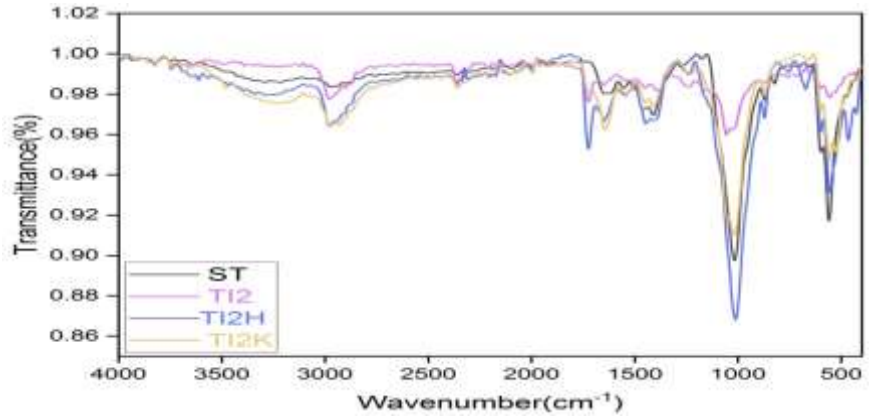

Fig (4) shows FTIR Analysis of nano- Titanium Dioxide concentrations of 2% + nano-paraloid concentration of 3% .

Conclusion

It is known that the archaeological bones are exposed to many damages due to the burial environment extracted from them or due to poor storage in the museum stores and the various effects of the factors of damage. And the effectiveness of this material in the processes of strengthening the archaeological bones, the compressive strength of samples reinforced with nano Titanium Dioxide material, there was an increase in the compressive strength of the TI2 reinforcement sample and the thermally aged and TI2H reinforcement sample. Chromatic change: The total chromatic change of the samples in ΔE occurred to a very slight and unnoticeable change occurred . Results of FTIR analysis , the chemical copmposition of samples that had been strengith with Nano Titanium Dioxide 2%, material not change in all the thermally and chemically aging samples , it can be seen that the functional groups of the phosphate and carbonate, the main component of hydroxyapatite, are not affected and there is no loss in any of constituent domains of these functional groups, and it can be observed the presence of the functional groups of the main component of collagen (Amide I Amide II, Amide A) in all samples compared to the standard sample .

References

1. Henriques DF, Nunes L, Brito J (2010); Performance of Paraloid B72 combined with the application of biocides on wood degraded by fungi. In: Proceedings of 4th international conference on wooden cultural heritage: interaction between wood science and conservation of cultural heritage, COST Action IE0601, Izmir Turkey.

2. Traistaru AAT, Timar MC, Campean M, Croittoru C, Sandu I (2012); Paraloid B72 Versus Paraloid B72 with nano-ZnO additive as consolidants for wooden artifacts. Mater Plast 49(4):293–300.

3. Clausi M, Crisci GM, Russa MF, Malagodi M, Palermo A, Ruffolo S. A, (2011); Protective action against fungal growth of two consolidating products applied to wood. J Cult Herit 12:28–33.

4. Pinto A. P. F, Rodrigues, J. D. (2008) Stone consolidation: The role of treatment procedures. Journal of Cultural Heritage, Vol. 9, pp. 38-53.

5. Cataldi, A., Dorigato, A., Deflorian, F., Pegoretti, A. (2014) Thermo-mechanical properties of innovative mi- crocrystalline cellulose filled composites for art protection and restoration. Journal of Materials Science, Vol. 49, pp. 2035-2044.

6. Del Grosso, C. A., Poulis, J. A., de la Rie, E. R. (2019) The photo-stability of acrylic tri-block copolymer blends for the consolidation of cultural heritage. Polymer Degradation and Stability, Vol. 159, pp. 31-42.

7. J., Leuninger, F., Tiarks, H., Wiese, B., Schuler, Wassrige Nano Komposite. Farbe & Lack 10/2004 S. 30 http://www.european-coating. com.

8. S. P., Koob (1986). The Use of Paraloid B-72 as an Adhesive: Its Application for Archaeological Ceramics and Other Materials, Studies in Conservation, 31 (1986) 7-14.

9. . P., Spathis, E., Karagiannidou, A. E., Magoula (2003). Influence of Titanium Dioxide Pigments on the Photo degradation of Paraloid Acrylic Resin, Studies in Conservation, 48, 57-64.

10. R. L., Feller (1984). Thermoplastic Polymers Currently in Use as Protective Coatings and Potential Directions for Further Research, ICCM Bulletin, 10, 5-18.

11. Technical Data Sheet: Paraloid B-72 Preservation Equipment Ltd, https://www. preservationequipment. com.

12. C. V., Horie, Materials for Conservation: Organic Consolidates, Adhesives and Coatings, Architectural press, Oxford, 1997.

13. La Russa, M. F., Rovella, N., de Buergo, M. A., Belfiore, C. M., Pezzino, A., Crisci, G. M., Ruffolo, S. A. (2016) ; Nano-TiO2coatings for cultural heritage protection: The role of thebinder on hydrophobic and self- cleaning efficacy. Progress in Organic Coatings, Vol. 91, pp. 1–8.

14. Manoudis, P. N., Gemenetzis, D., Karapanagiotis, I. (2017); A comparative study of wetting properties of a superhydrophobic siloxane material and rose petal, Scientific Culture, Vol. 3, No. 2, pp. 7-12.

15. Chatzigrigoriou, A., Manoudis, P. N., Karapanagiotis, I. (2013); Fabrication of Water Repellent Coatings Using Waterborne Resins for the Protection of the Cultural Heritage, Macromolecular Symposia, Vol. 331-33 (1), pp. 158–165.

16. Scalarone, D., Lazzari, M., Chiantore, O. (2012); Acrylic protective coatings modified with titanium dioxide nanoparticles: Comparative study of stability under irradiation. Polymer Degradation and Stability، Vol. 97, pp. 2136-2142.

17. X. Y. Wang, Y. Zuo, D. Huang, x. d. Hou, and Li. Y. Boa, " Compartive Study on Inorganic Composition and Crystallographic Properties of Cortical and Cancellous Bone, Biomedical and Environmental Sciences 23, 2010, pp.473-480.

18. J. C. Hiller, T. J. U. Thompson, M. P. Evison, A. T. Chamberlain, T. J. Wess, " Bone mineral change during experimental heating: an X-ray scattering investigation. Biomaterials 24. 2003, pp.5091-5097.

19. N. Kalsbeek, and J. Richter, Preservation of burned bones: an investigation of effects of temperature and PH on hardness, Studies in conservation, Vol.51, No.2, 2006, pp. 123-138.

20. M. M. Figueiredo, A. Fernando, G. Martins, J. Freitas, F. Judas, and H. Figueiredo, " Effect of the calcination temperature on the composition and microstructure of hydroxyapatite derived from human and animal bone, Ceramics international 36, 2010, pp.2383-2393.

21. G. Abdel-Maksoud," Comparison between the properties of "Accelerated Aged" bone and archaeological bones, Journal of Mediterranean archaeology and archaeometry, Vol.10 (1),2010, pp. 89-112 .

22. M. M. Figueiredo, J. A. F. Gamelas, and A. G. Martins, " Charachterization of bone abd bone-based graft materials using FTIR Spectroscopy, Infrared spectroscopy – life and biomedical sciences(Portugal), 2012, pp.316.338.

23. G. T. Walker, " The mechanical properties of artificially aged bone: probing the nature of the collagen-mineral bond, palaeogeogrphy,palaeoclimatology,palaeoecology 310, 2011. Pp.17-22.

24. Mohamed Moustafa Ibrahim , Wael Sabry Mohamed, and Hamdy Mohamed Mohamed, (2021) ; EXPERIMENTAL STUDY FOR EVALUATION OF PARALOID® B72 AND ITS NANOCOMPOSITE WITH NANO TiO2 AND NANO ZnO FOR CONSOLIDATION OF POTTERY SAMPLES, SCIENTIFIC CULTURE, Vol. 7, No. 2, pp. 101-111.

25. A. B. Oyedeji , O. P. Sobukola, E. Green1 & O. A. Adebo " Physical properties and water absorption kinetics of three varieties of Mucuna beans, Scientific Reports 11, 2021, p.5450. https://doi.org/10.1038/s41598-021-85087-8 .

26. E. A. Baryeh, " Physical properties of bambara groundnuts", J. Food Eng. 47(4), 2001, pp. 321–326.

27. M. Awad & A. Al-Humaidhi, " Engineering methods for measuring the physical and mechanical properties", water content, and flow rates of underground rocks containing water, the first symposium for rationalizing water consumption and developing its sources, Riyadh, Saudi Arabia(1421 AH).

28. E. P. Kearsley and P. J. Wainwright, " Porosity and permeability of foamed concrete" ,‖ Cement and Concrete Research,. vol. 31, no. 5, 2001, pp. 805-812.

29. R. Shabbar, P. Nedwell, and Z. Wu, " Porosity and Water Absorption of Aerated Concrete with Varying Aluminium Powder Content", International Journal of Engineering and Technology, Vol. 10, No. 3, 2018, PP.234-238. DOI: 10.7763/IJET.2018.V10.1065.

30. K. J. Klabunde, R. S. Mulukutla, (2001) ; "Chemical and Catalytic Aspects of Nanocrystals", In:Nanoscale Materials in Chemistry, Edited by K. J. Klabunde, John Wiley and Sons, Inc. Kansas, PP.232-261.

31. J. I. Morán, V. A. Alvarez, V. P. Cyras, & A. Vázquez, (2018); " Extraction of cellulose and preparation of nanocellulose from sisal fibers". Cellulose, 15, PP.149–159.

32. N. H. El-sayed , et al, (2020); "Preparation and characterization of Paraloid B-72/TiO2 nanocomposite and their effect on the properties of polylactic acid as strawberry coating agents" , Journal of Food Saftey, Wiley Periodicals LLC, pp.1-14.

33. Wenjuan Li , Junling Lin , Yaru Zhao and Zihe Pan, (2021) ; The Adverse Effects of TiO2 Photocatalycity on Paraloid B72 Hybrid Stone Relics Protective Coating Aging Behaviors under UV Irradiation, Polymers, 13, 262, PP.1-15 .

34. M.M. Figueiredo, J.A.F. Gamelas and A.G. Martins (2012). Characterization of Bone and Bone-Based Graft Materials Using FTIR Spectroscopy, Infrared Spectroscopy - Life and Biomedical Sciences, Prof. Theophanides Theophile (Ed.),pp.315-338. ISBN: 978-953-51-0538-1.

35. Fleet, M. E. (2009). Infrared spectra of carbonate apatites: ν2-Region bands. Biomaterials, 30(8), pp. 1473-1481.

36. Landi, E. (2003). Carbonated hydroxyapatite as bone substitute. Journal of the European Ceramic Society, 23(15), pp. 2931-2937.

37. Verdelis, K., Lukashova, L., Wright, J. T., Mendelsohn, R., Peterson, M. G. E., Doty, S., et al. (2007). Maturational changes in dentin mineral properties. *Bone, 40*(5), pp. 1399-1407.

38. Chang, M. C., & Tanaka, J. (2002). FT-IR study for hydroxyapatite/collagen nanocomposite cross-linked by glutaraldehyde. Biomaterials, 23, pp. 4811–4818.